Modular Auger Design to Prevent Clogging in Suction

by

Travis Leathrum

Submitted to the
Department of Mechanical Engineering
in Partial Fulfillment of the Requirements for the Degree of

Bachelor of Science in Mechanical Engineering

at the

Massachusetts Institute of Technology

June 2019

Signature of Author: **Signature redacted**

Department of Mechanical Engineering
May 20, 2019

Certified by: **Signature redacted**

Alexander Slocum
Walter M. May and A. Hazel May Professor of Mechanical Engineering
Thesis Supervisor

Accepted by: **Signature redacted**

Maria Yang
Associate Professor of Mechanical Engineering
Undergraduate Officer

1

Modular Auger Design to Prevent Clogging in Suction

by

Travis Leathrum

Submitted to the Department of Mechanical Engineering
on May 20, 2019 in Partial Fulfillment of the
Requirements for the Degree of

Bachelor of Science in Mechanical Engineering

ABSTRACT

A mechanical design was conducted for a modular auger system that reduces the risk of clogging in suction piping meant to process sargassum seaweed. The auger supports a slurry pump-based system being designed to address sargassum blooms adversely affecting beaches in the Caribbean. By reducing clogging, the auger will prevent damage to the pump and reductions in productivity. A mathematical model of the auger system was created, then a small-scale physical model was built to test the concept. These tests exposed flaws in the mechanical details of the design, but the viability of the concept was shown, so a full-scale design was completed to be implemented as a backup in an extended field test that will be conducted in the Caribbean during the summer 2019.

Thesis Supervisor: Alexander Slocum
Tile: Walter M. May and A. Hazel May Professor of Mechanical Engineering

Acknowledgements

I would like to express my deepest thanks to my thesis supervisor, Professor Slocum, as well as Master's student, Luke Gray, for the opportunity to work on this project this semester and all of the help they offered me along the way. It was a great learning experience and I wish I had more time to continue working on it this summer. Luke consistently helped me through every step in the research and thesis process. I would have been lost without him.

I would also like to thank Val Peng and the other students in the Precision Engineering Research Group for the help they offered me throughout the testing process. Val especially helped me a lot with the hydraulic motor selection and the setup of the physical tests. PERG provided me with a great community in which I learned a lot this past year. I would also like to thank Hayami Arakawa and the MIT Hobby Shop for help machining all of the custom parts of the physical model I built.

Finally, I'd like to express my appreciation for all of my friends and family for all of the support they gave me throughout my time at MIT. They all played a part in helping me get through my toughest times, and I would not have been able to get this far without them.

Table of Contents

List of Figures

List of Tables

1. Introduction

Sargassum is an invasive species of seaweed algae that has begun covering beaches of the Caribbean in recent years. It blooms in large mats that float on the surface of the ocean and frequently wash ashore. These large piles of brown algae have made otherwise pristine beaches unappealing to tourists and have negatively impacted the ecology of island nations in the region. These expansive mats of seaweed block sunlight from reaching shallow-water vegetation, effectively starving coral reefs. When sargassum washes ashore, it dies and as it decays, it releases foul-smelling fumes that cause nausea and respiratory problems. The decaying sargassum also causes eutrophication, which suffocates animals living in the affected areas. Currently, residents collect and dispose of the dead sargassum once it is on shore, which is slow and does not actually solve most of the aforementioned issues. A solution to prevent sargassum from making landfall is urgently needed. Master's student Luke Gray and Prof. Alexander Slocum, of the MIT Precision Engineering Research Group have developed a system called "Sargassum Ocean Sequestration" ("SOS") which seeks to remove sargassum from the open ocean. This system pumps sargassum out of the ocean and down to a depth at which hydrostatic pressure crushes the buoyant bladder of the sargassum, making it negatively buoyant so that it sinks to the ocean floor. This would get rid of large quantities of sargassum without having to collect, store or process the sequestered sargassum. Refer to Luke A. Gray's thesis [1] for extensive background on this system.

Figure 1-1: Photograph of sargassum washing ashore in Florida [2]

In any solids pumping system, it is paramount to prevent clogging. Clogs in suction piping cause interruptions in operation and can damage the pump by inducing cavitation. Clogs in suction piping obstruct the flow that reaches the pump, lowering the water pressure around the impeller. If this pressure reaches the vapor pressure of water at the ambient temperature, the water boils, causing the immediate implosion of vapor bubbles, resulting in shockwaves that can damage the impeller and its housing. Clogging of the suction pipe leading to the pump is the single most lethal risk to the success of the SOS concept. To ensure clogging does not occur, a modular auger device is hereafter designed to:

1. Catch biomass that would otherwise cause clogs in the suction piping, and

2. Slowly meter these solids into the suction piping.

Specifically, if a clump of particularly high volumetric solids concentration (40-90%) enters the pipe, the auger rotation will regulate the solids flow to a manageable amount (around 30%) in order to ensure that the pipe does not clog downstream. An auger provides the added benefit of breaking up the conveyed solids.

Three different inlet devices are currently being investigated, so for testing, the auger design needs to be modular such that it can be implemented with each inlet device without permanent installation. The auger needs to be able to be installed and removed easily from each device while in the field.

One of these inlet designs called a sump is similar to a bucket which is held just under the surface of the ocean with the pipe inlet pointed down inside. Water flows over the edge and into the sump, pulling sargassum with it. Another device consists of a plaining vee which is mounted on outriggers such that as the boat drives through a mat of sargassum, it skims the ocean surface, collecting sargassum and pushing it into the inlet of the pipe. Another design in development consists of a floating buoy with an array of holes pointed down into the water. The sump and buoy designs rely on a boom that surrounds a large mat of sargassum and pulls it in toward the inlet.
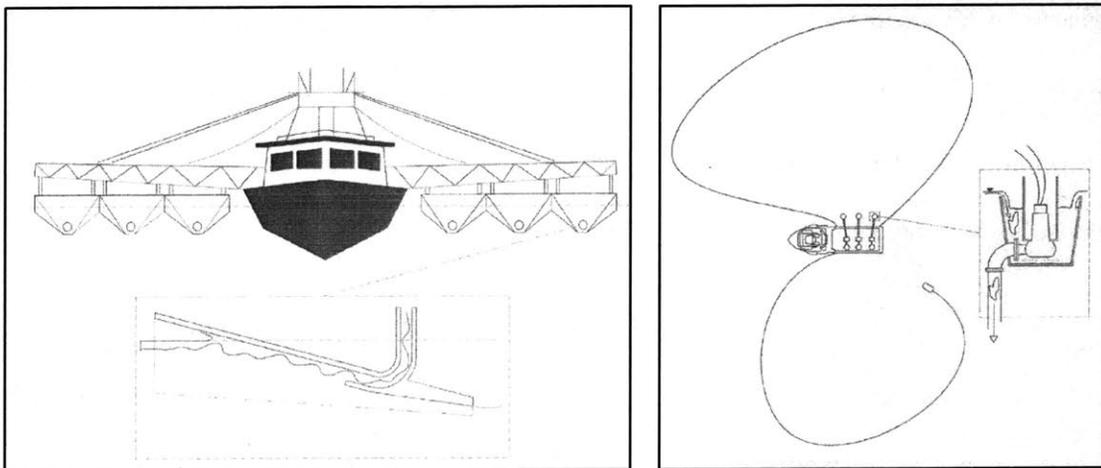
Figure 1-2: Basic conceptual sketches of the vee device with corresponding outriggers (left) and sump with corresponding encircling boom schematic (right). These designs are still in development and will look much different from this in the end, but this conveys the basic concepts of the two designs. [1]

This summer 2019, a 20-day, large scale test of the complete system is to be conducted on a pilot vessel in the Caribbean. This system will include a 5000 gallon per minute (GPM) pump, 12" piping, and all three inlet devices. An auger of this scale must be designed to be utilized in this system. This will help to determine how the device scales with the size of the pipe and pump and will test how well it performs in long-term operation. To test the basic concept, a small scale test was conducted in a pond with 427 GPM pump and 4" pipe.

Auger screws have been used for centuries in the processing of bulk goods and organic matter. However, augers, especially one that must survive sustained, harsh operating conditions, require careful analysis and testing. First and foremost, it is critical that this device does not, itself, present a clog risk. Therefore, both a shafted and a shaft-less auger were designed to be tested inside the pipe at the inlet.

An auger with a large inner diameter and no shaft up the center allows water and sargassum to flow without having to wind through the flights around the entire length of an ordinary shafted auger. This also allows the flow to be broken up into flow through the center of the auger and flow that is released from the auger as it turns. This enables it to decrease the flow rate of solids without significant pressure losses in the pipe.

A first order model was developed to predict the auger's performance and deterministically design parameters. Then a solid model was built and tested to evaluate the design model and identify other outstanding risks.

2. Analysis

2.1 First Order Model and Assumptions

An equivalent fluid model, wherein the density of the incompressible, irrotational, equivalent fluid are the weighted averages of the respective solid and liquid properties, was assumed for the purposes of hydraulic calculations. In his experiments on the behavior of sargassum, Gray determined that the addition of sargassum does not significantly impact the viscosity of the slurry, so the viscosity is assumed to be equal to that of water [1].

One major defining characteristic of a slurry flow state is its volumetric solids concentration, C_v [3]. The volumetric solids concentration of a slurry is defined in terms of the volumetric flow rates of the solid and the liquid, Q_S and Q_L respectively, by Equation 2.1:

$$C_v = \frac{Q_S}{Q_S + Q_L} \qquad \text{2-1}$$

Where Q_S refers to the volumetric flow rate of the solid (sargassum) and Q_L refers to the volumetric flow rate of the liquid (water). One goal of this machine is to decrease the C_v, and in order to do this, the Q_S must be decreased without significantly lowering the Q_L.

The governing equations for changes in C_V are two separate conservations of momentum of the liquid and the solid. These are expressed in Equations 2.2 and 2.3 respectively where x refers to length in the pipe, c refers to the solids concentration at a particular point in the flow and v_S and v_L refer to the velocities of solids and liquids [3].

$$\frac{\partial c}{\partial t} + \frac{\partial c \rho_S v_S}{\partial x} = 0 \qquad \text{2-2}$$

15

$$\frac{\partial(1-c)}{\partial t} + \frac{\partial(1-c)\rho_L v_L}{\partial x} = 0 \qquad\qquad 2\text{-}3$$

In order for the concentration of solids to vary across the length of the pipe, it must also vary in time. This is to say that an equilibrium cannot be reached in which the $C_{v\,out}$ is maintained lower than the $C_{v\,in}$ without an increasing C_v inside the pipe. You can only maintain a metered C_v as long as you have somewhere to hold it within the pipe.

When a clump of high C_v sargassum enters the pipe, some of the sargassum gets caught on the auger flights due to friction such that for a limited time, the C_v advancing through the pipe past the auger is lower than the C_v at the entrance. Since the auger is moving, the deposited sargassum is gradually released, while some of it is pushed around the flights into the central flow. A pile forms behind each flight and eventually the volume behind each flight fills up such that the rate of sargassum deposited is the same as the rate at which it is released. At this point, the C_v reaches equilibrium and the C_{vout} equals C_{vin}.

The auger is able to do this by catching sargassum behind each flight and slowing it down, while the water flows around it more easily. It is able to maintain a lower C_v for a limited time before the volume of the flights becomes saturated with sargassum and it reaches an equilibrium at which the $Q_{S\,in} = Q_{S\,out}$.

The more volume the auger can hold, the larger the clump it can handle while still metering the $C_{v\,out}$ before it reaches that equilibrium. The maximum volume the auger can hold can be calculated using Equation 2-4 in which n is the number of flights, D_{out} is the outer diameter of the auger (the inner diameter of the pipe), D_{in} is the inner diameter of the auger and b is the thickness of the pile of sargassum built up behind the auger flights.

$$V_{max} = bn\frac{\pi}{4}(D_{out}^2 - D_{in}^2)$$ 2-4

The volumetric rate at which sargassum enters the pipe is defined as $Q_{S\,in}$, and the rate at which it is pushed along the flights and released from the end of the auger is defined as $Q_{S\,aug}$ which is calculated using Equation 2-5 where ω refers to the angular velocity of the auger.

$$Q_{S\,aug} = b\omega A_{aug}$$ 2-5

The time it takes to fill and empty the auger are expressed in Equations 2-6 and 2-7 respectively in which v_{ave} is the average velocity of the total flow through the center of the pipe.

$$t_{fill} = \frac{V_{max}}{A_{aug}(v_{ave} - b\omega)}$$ 2-6

$$t_{empty} = \frac{n}{\omega}$$ 2-7

2.2 Frictional Analysis for Determination of Auger Pitch

When sargassum is caught behind an auger flight, it is held in place by friction between the auger and the algae. To find an optimal auger pitch, the simplified free body diagram shown below in Figure 2-1 was created in which the only forces acting on a particle of sargassum are the drag force, F_D, caused by the flow of water around it, the normal force, F_N, and the friction force, F_f, from the auger as a result of the drag force. The actual physics at hand are much more complicated since the flow is not one-dimensional or laminar and sargassum is not comprised of simple spherical particles with uniform friction and drag behavior. The drag forces are dependent on the relative velocity between the flow and the auger, which is expressed in Equation 2-8, but it is not necessary to calculate F_D for optimizing the pitch.

17
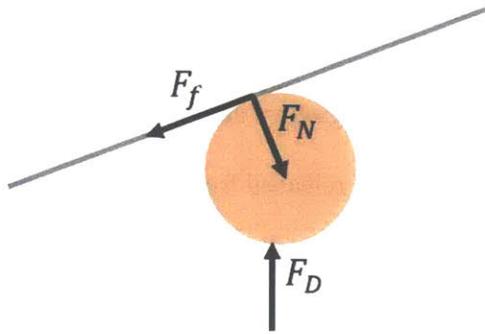
Figure 2-1: Free body diagram illustrating the forces acting on a sargassum particle. F_D refers to the drag force from the water flow. F_N is the normal force acting on the sargassum from the auger flight. F_f is the friction force resulting from the contact between the auger and the sargassum.

$$v_{rel} = v_{ave} - \omega p \qquad\qquad 2\text{-}8$$

The normal force and friction force are proportional to the ratio between the auger pitch, p, and pipe inner diameter, D, as shown in Equation 2-9 and 2-10.

$$F_N = 2F_D \frac{D}{p} \qquad\qquad 2\text{-}9$$

$$F_f = 2\mu_d F_D \frac{D}{p} \qquad\qquad 2\text{-}10$$

Using this, Newton's Third Law is applied to the force balance between the friction and the drag along the axis parallel to the auger flight in Equation 2-11.

$$\sum F = F_D \frac{p}{\pi D} - F_f = 0 \qquad\qquad 2\text{-}11$$

From this, a relationship was found between the pitch, pipe diameter, and the dynamic coefficient of friction between the particle and the auger to ensure that the auger can catch sargassum. The sargassum catches if the friction force outweighs the drag pushing it along. This inequality is expressed in Equations 2-12 and 2-13.

$$F_D \frac{p}{\pi D} < \pi \mu_d F_D \frac{D}{p} \qquad \text{2-12}$$

$$p < \pi D \sqrt{\mu_d} \qquad \text{2-13}$$

A value for μ_d was not available, but if it is less than 0.1, then the pitch needs to be smaller than the diameter. In order to catch the maximum amount of sargassum, the system must have more friction than drag, so you want to maximize the ratio of diameter to pitch without impacting the other factors at hand, like pressure losses. As such, for the physical model, an auger with pitch equal to half the diameter was selected.

It is quite difficult to calculate an exact amount that would build up in the auger (expressed as b in Equation 2-4), since there are some very complicated dynamics at play in non-homogenous slurry flow. Engineers have not been able to accurately characterize the rate of deposit in slurry flow, so they use correlations from data instead, but these correlations have at best ± 20% certainty [3]. This data was collected by studying slurry flow in simple pipes with no obstructions. The deposit dynamics at hand with an auger in the pipe are even more complicated, so this data would not directly correlate to the behavior in this system, but some useful conclusions can be drawn from them.

The most useful observation from this is the minimum velocity at which particles settle in a pipe. Settling in this case is caused by gravity pushing particles into the pipe such that friction against the pipe overcomes the drag forces caused by the flow around them. This situation is not what would happen in an auger, but there is likely a minimum velocity at which deposition occurs in the auger as well. This would suggest that a lower relative velocity between the flow and the auger would be advantageous. This is not to say that one should just run the auger close to the speed of flow, because that would push out sargassum too quickly, causing the pipe to clog

downstream. The auger will also induce a centrifugal flow which will repel solids if it spins too fast. The driving factor for the motor speed should be the desired solids concentration output in response to clogs.

2.3 Plug Model for Determination of Motor Speed

When a large enough clump is introduced, the auger fighting will fill up and the material flowing through the center will catch on the sargassum stuck behind the flights, causing it to build up in the center. This sargassum forms into a plug that is pushed forward by the auger, so a different model must be used until the plug is either broken up by the flow behind it or released out the end of the auger. In this model, the flow is treated as a uniform cylinder of concentrated sargassum that moves at the linear rate of the auger as shown in Equation 2-14.

$$v_{plug} = p\omega \qquad\qquad 2\text{-}14$$

The volumetric flow rate of solids leaving the auger is then

$$Q_{S\,plug} = p\omega A_{pipe} \qquad\qquad 2\text{-}15$$

This cylinder is porous, so it is assumed that some water would still be able to flow through the clogged section. By plugging this $Q_{S\,plug}$ into Equation 2-1 along with the flowrate of the pump, the solids concentration coming out of the pipe can be found for this case. The resulting Equation 2-16 can be rearranged to calculate the motor speed, ω, needed to get the desired C_v as shown in Equation 2-17. The speed of the auger must be informed by this analysis to ensure a metered flow that won't clog the pipe downstream in the case of a clog in the auger.

$$C_v = \frac{p\omega A_{pipe}}{Q_T} \qquad\qquad 2\text{-}16$$

20

$$\omega = \frac{C_v Q_T}{p A_{pipe}} \qquad\qquad 2\text{-}17$$

For the sake of testing, the target C_v was 30%. The flow rate, Q_T, of the pump that was used was 427 GPM. This along with the previously determined p and area of a 4 inch pipe, the desired angular velocity was found to be around 300 RPM.

This model can be improved by calculating the change in liquid flow rate, Q_L, as a result of this buildup of sargassum. This can be done using Darcy's Law shown in Equation 2-18. The liquid flow rate is dependent on the permeability of sargassum, k, and the pressure drop across the plug, Δp. As such, the fluid flow rate cannot be found without measuring these two values empirically. Future work should seek to measure these values for a plug in the auger.

$$Q_L = -\frac{kA\Delta p}{\mu L} \qquad\qquad 2\text{-}18$$

2.4 Pressure Loss Analysis

An essential requirement for the auger is that it does not cause too much loss of pressure. If the auger introduces too much minor losses, then it only increases the risk of cavitation. The flights of the auger create significant turbulence in the flow around it. In order to model this effect, each flight of the auger is treated as a thin orifice. This is a very conservative model. An auger would realistically cause less head loss than a series of orifices, since the turbulence is spread out along the screw pitch. The minor losses due to each orifice are calculated using Equation 2-19, where D_1 is the inner diameter of the pipe, D_2 is the inner diameter of the auger (reference figure here), and Re is the Reynolds number [5].

$$K_{orifice} = \left[2.72 + \left(\frac{4000}{Re} \right) \left(\frac{D_2}{D_1} \right)^2 \right] \left[1 - \left(\frac{D_2}{D_1} \right)^2 \right] \left[\left(\frac{D_1}{D_2} \right)^4 - 1 \right] \qquad 2\text{-}19$$

21
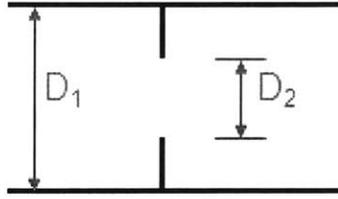
Figure 2-2: Diagram of the orifice geometry. Note that D_1 refers to the outer diameter, and D_2 refers to the inner diameter of the auger [6]

There are also minor losses caused by any elbows in the pipe (K_{elb}= 0.5) and the inlet (K_{ent}= 0.78). The entrance was treated as a protruding inlet. The pressure head losses (Δh_m) due to each minor loss element are then calculated using Equation 2-20 where V is the mean velocity and g is the acceleration due to gravity. The pressure losses can then be found using Equation 2-21.

$$\Delta h_m = K \frac{V^2}{2g} \qquad \text{2-20}$$

$$\Delta P = \rho K \frac{V^2}{2g} \qquad \text{2-21}$$

For the auger used in testing, the $K_{orifice}$ is equal to 1.06, so the pressure loss due to each flight is 2.55 psi. The auger was 10 flights long, so the total pressure loss due to minor losses in the auger was 25.5 psi. This was determined not to cause cavitation using the Bernoulli Equation. By multiplying this value by the area of one flight, one can also find the axial load applied to the auger, which is equal to 240.3 lbs. This is the axial load that the ball bearing at the base of the auger must be able to hold. Future work should seek to measure the pressure loss across the auger, since this orifice model is most likely inaccurate. This same experiment should also measure the pressure losses in the plug case as another cavitation risk.

3. Mechanical Design of Physical Model

This section discusses the general mechanical design of the auger system and the specifics of the prototype which was built and tested during the 2019 spring semester. The system consists of an auger screw, a suction pipe (which also provides the bearing surface for the auger), and a hydraulic motor, the design and selection of which are described below. Refer to Figures 3-1 and 3-2 for how these parts fit together in the assembly. Refer to the bill of materials, Table 3-1 in section 3.4 for the price, source, and part numbers of all parts discussed in this design. The development of this model involved two iterations, the first of which was built quickly, cutting a few corners in the mechanical design to save time. As a result, it failed in testing, so several changes informed by peer review were made to the design. The end result was a much more robust, well-rounded machine. This served as a valuable learning experience which will be discussed later in this section.
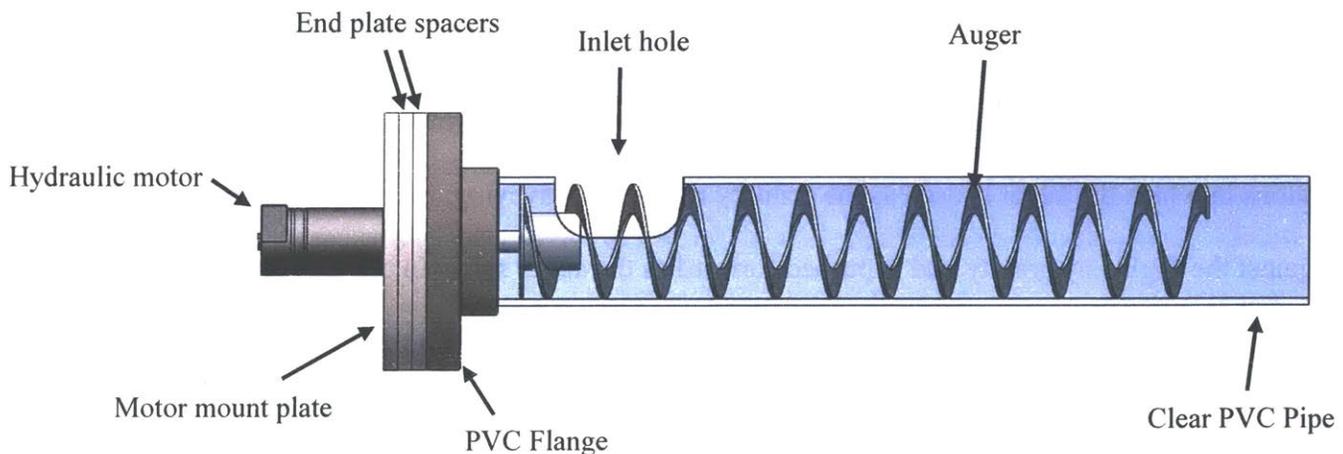
Figure 3-1: Labeled CAD model showing the auger assembly from the side. The pipe leading to the pump is connected to the right side of the PVC pipe.
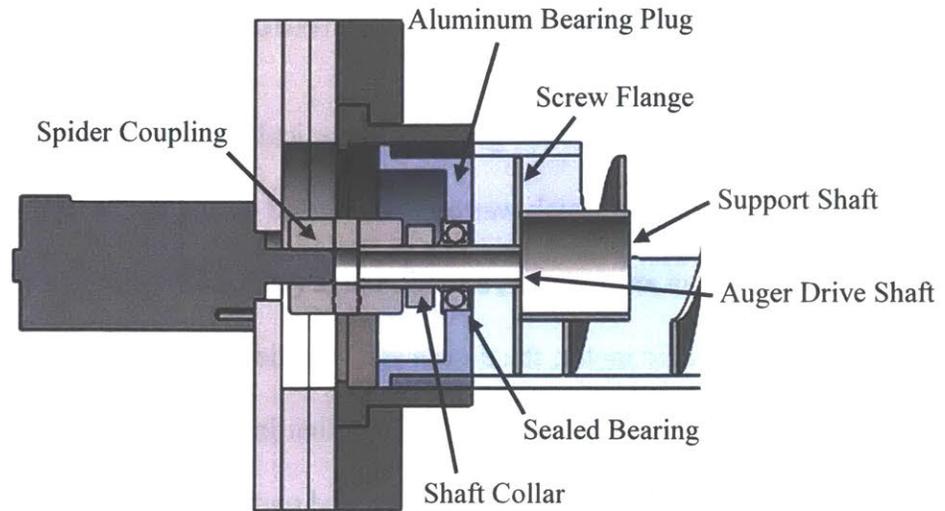
Figure 3-2: Labeled Cross Sectional View of the CAD model

3.1 Auger Design and Fabrication

An auger was chosen for its ability to provide metered flow even in extremely high

concentrations of solids. Two types of augers were investigated for this project: shafted and

shaftless augers. As the name suggests, shaftless augers do not contain a shaft through the center

of the flighting. This leaves a space in the center that material can flow through. For usual

applications in which the auger is used as the primary means of conveying, the material is held

back against the flights by gravity and is pushed forward as the auger spins. In this application,

the auger is not the dominant force acting on the material. The flow is driven entirely by the

pump, and the auger only slows the sargassum. The sargassum is pushed up against the back of

the flights and is allowed to move forward by the auger spinning. In a shaftless auger, most of

the flow is allowed to move straight through the center of the screw, so it experiences less

pressure loss than a shafted one. Under low-concentration conditions, the auger does not catch

much sargassum and most of it is able to flow quickly through the center of the screw. It is only

24

when a large quantity of high-concentration sargassum enters the inlet that the auger greatly impacts flow. In this state, sargassum collects on the flights and is metered out the end by the movement of the auger while water is still able to flow through the center.
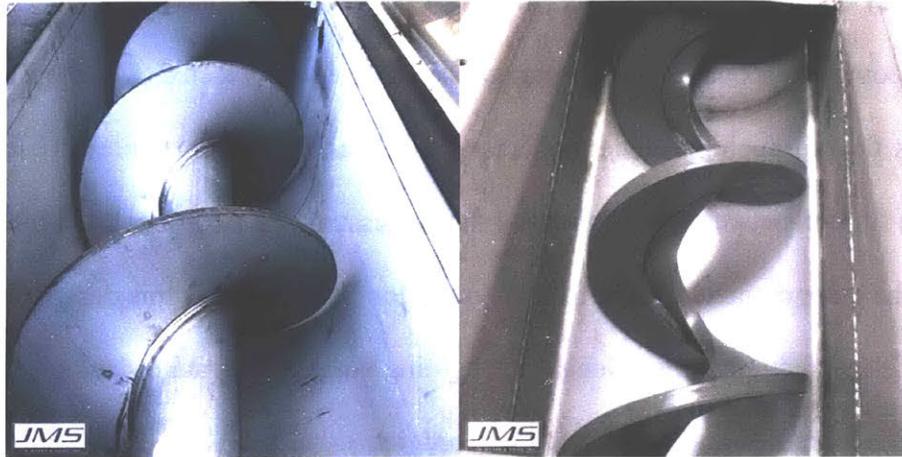
Figure 3-3: Photographs of a shafted auger (left) and a shaftless auger (right) [8]

In order to avoid pressure losses, the pipe diameter must be constant throughout the system, including the section with the auger in it, so the outer diameter of the auger must be equal to the diameter of the pump inlet. The scale selected a 4 inch inlet was used, so the auger and pipe were designed to have this same diameter. The pitch of the auger is driven by Equation 2-13 in the Analysis section which tells us that the pitch should be lower than the pipe diameter to ensure enough friction to catch the sargassum. The inner diameter must be large enough that at any given point along the pipe, the majority of the flow moves around the flight such that the model described in the Analysis section holds. The length of the auger dictates the size of clump that the system is able to handle. In order to meter flow for larger clumps, a longer auger is desirable, but this length is limited by the stress on the auger, the pressure losses induced, and the geometric constraints of the straight pipe length.

Access to proper screw flight forming tools was not available, so making the auger would have been difficult and would produce a low-quality screw. Instead, the auger flighting was purchased from a manufacturer that sells replacement flighting for augers. Their selection was limited, but they offered several options with a 4" outer diameter, allowing selection of an appropriate geometry. The largest inner diameter available was selected (2") to ensure that the model of bulk flow through the center holds for this test and to minimize pressure loss. To maximize the friction between the flights and the sargassum, the auger needed a pitch length shorter than the outer diameter. Refer to section 2.2 for elaboration on this design decision. To fulfill both of these requirements, a length of flighting made of 10-gauge steel with a 4" outer diameter, 2" inner diameter, and a 2" pitch was ordered.
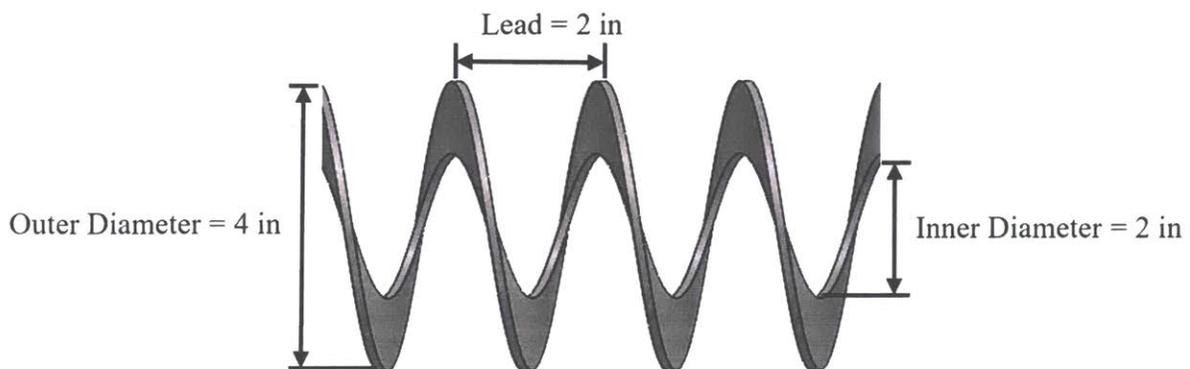
Figure 3-4: Labeled CAD model of the auger flighting showing what is meant by the terms inner diameter, outer diameter, and pitch.

This flighting was fixed to a 0.75" OD steel drive shaft via welding to a circular flange on the end of the screw near the inlet. This flange was a simple circle cut out of a 10-gauge steel plate. A long 2" wide tube was fit through the center of the screw, keeping it straight and concentric. Two small disks that fit around the outside of the shaft and the inside of the 2" tube were used to center the tube on the axis of the drive shaft, and the assembly was welded together

at the base of the screw. For the first iteration, the auger was welded to the flange by the end of flighting alone, but after peer review, this was determined to be too small of a weld line (only 1 inch long). This joint did not fail in testing, but it was a potential failure point with a simple solution. To strengthen that weld joint, a short length of the 2" diameter tube (with length equal to one screw pitch) was welded to the inside of the screw at the end against the flange. This support tubing provided much more contact area for a much stronger weld joint.
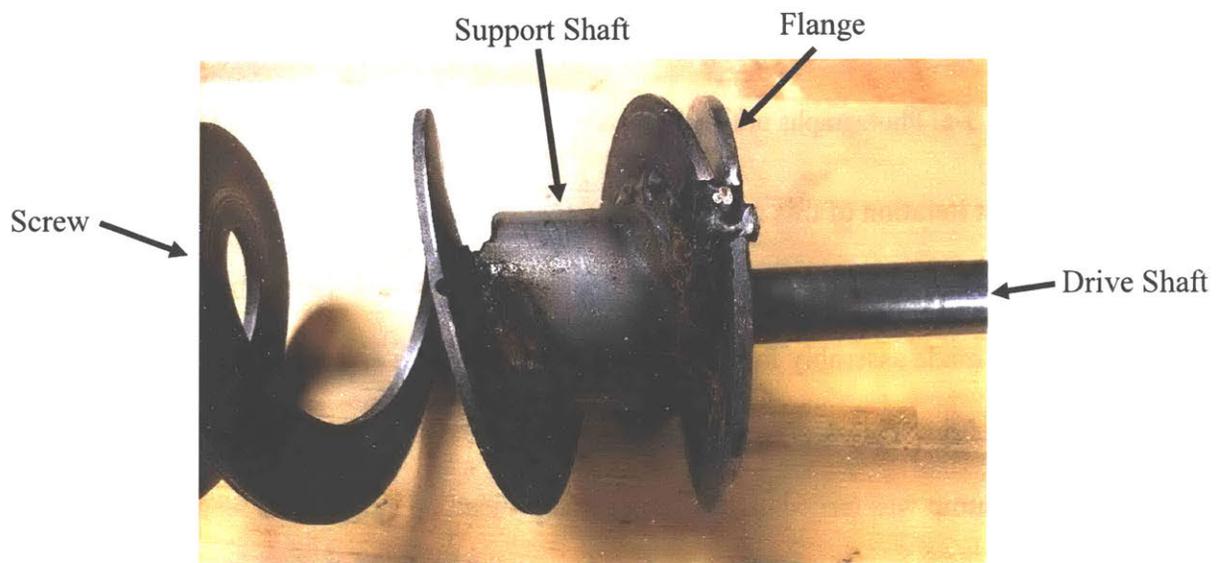
Figure 3-5: Labeled photograph of the base of the shaftless auger. Not the support shaft that was welded to the flange and the screw. The auger is driven by a motor coupled to the drive shaft on the right.

A second screw-shaft assembly was welded together with a 2" wide tube running through the entire length of the screw, welded regularly across its length. This shafted auger was made to support testing how the system would behave with a shafted auger in case the model for the shaftless auger was proven not to work. The shaft took out all of the compliance in the geometry of the screw and made it virtually rigid. If the deformation of the shaftless auger proved to be problematic, then this shafted auger could turn out to be valuable. It served as a baseline to compare performance and test the hypothesis that a shaftless auger would provide better flow.

27
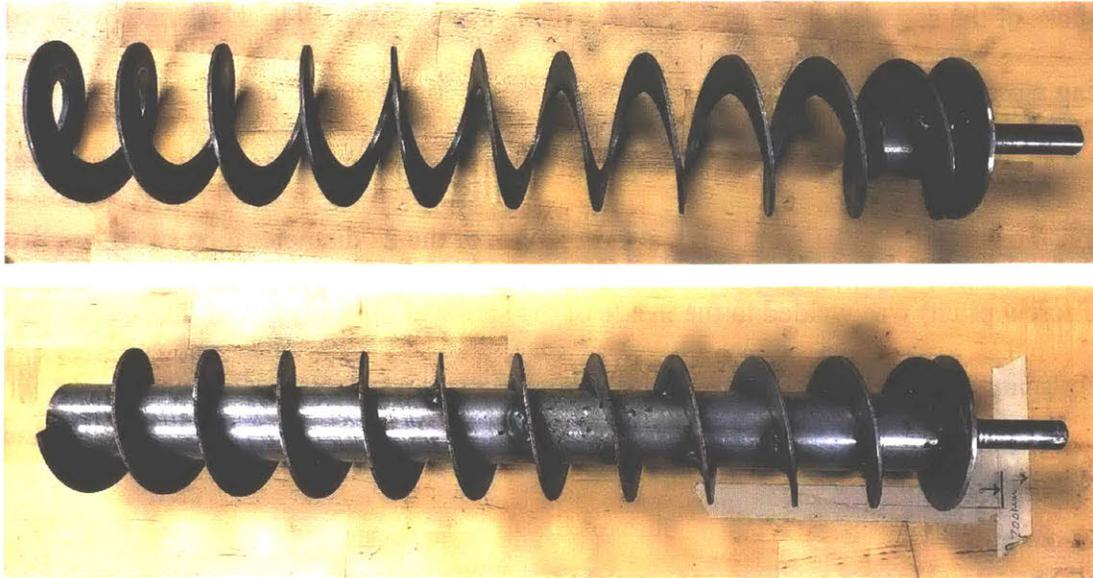
Figure 3-6: Photographs of the shaftless (top) and shafted (bottom) auger modules.

In the first iteration of this machine, the auger was axially constrained by a thin HDPE ring fixed to the inner wall of the pipe at the open end of the screw. This solution was easy to manufacture and made assembly fast and easy, but it caused the entire machine to fail when exposed to water flow. This design did not account for the compression of the auger as a result of drag. When the pump was turned on, the auger was pressed up against this feature, and it compressed like a spring far enough to disengage the spider coupling, so that it stopped turning. This proved that the auger needs to be fully, properly constrained on the other end near the motor.

Through peer review, it was decided that the auger would be constrained axially by a collar fixed to the shaft near the coupling which would transmit axial loads to a ball bearing. This bearing was press fit into an aluminum plug which slides into the end of the PVC pipe with a running fit. This plug has a flange that presses against the end of the pipe to hold it in place. Figure 3-7 below shows how this part transmits force from the auger to the pipe.

Force transmitted from the shaft collar to the bearing

Drag on Auger

Force transmitted from the bearing housing to the pipe

Radial constraint of the auger
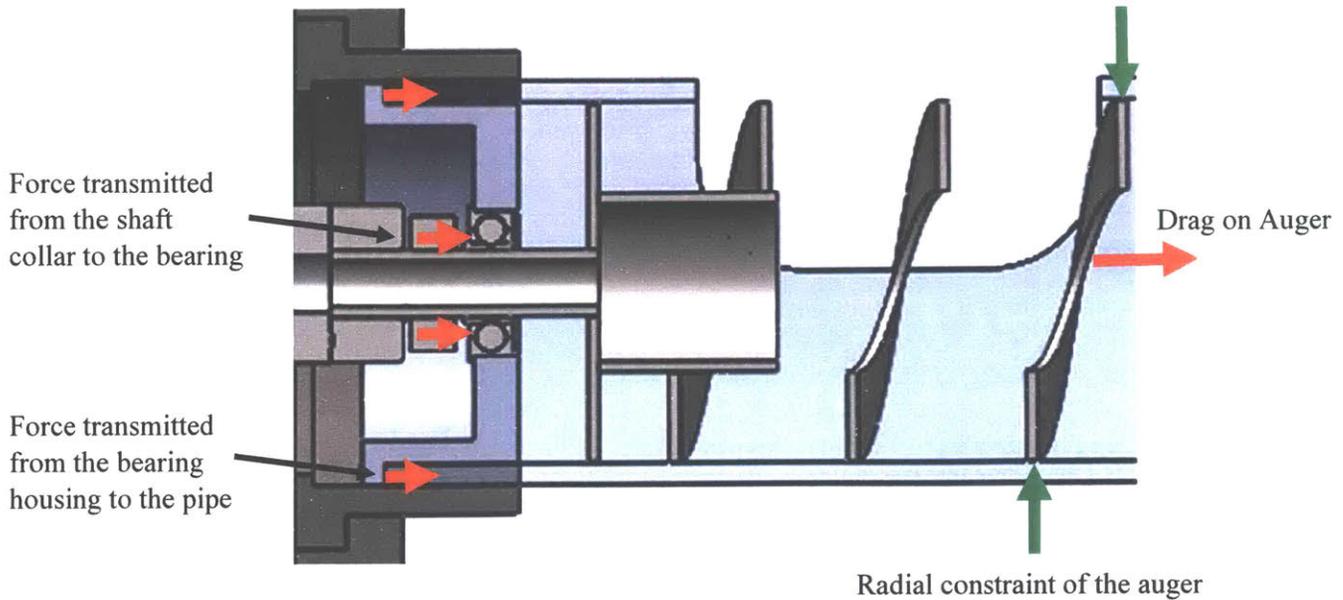
Figure 3-8: Force Diagram showing how the auger is constrained within the pipe. Note that the shaft collar, which is fixed to the shaft, transmits the axial load from the auger to the bearing, which transmits that force to the pipe via the flange in its housing.

A lubricated, sealed deep-groove ball bearing was selected for their resistance to lubrication losses in water. These bearings are not perfectly sealed, so they will gradually lose the grease keeping them lubricated, shortening their life. This was not a concern due to the short duration of the underwater tests, but the bearing life will be a concern moving forward. Deep groove ball bearings have an axial load capacity approximately equal to their radial load capacity. The expected load on the auger per flight is calculated by multiplying the pressure loss on each flight (Equation 2-20) by the area of said flight. The total axial force on the auger used in testing was estimated to be 240 lbs. The bearing selected is rated for 1300 lbs. so there was a safety factor of 5.4 which is more than sufficient for these short term tests.
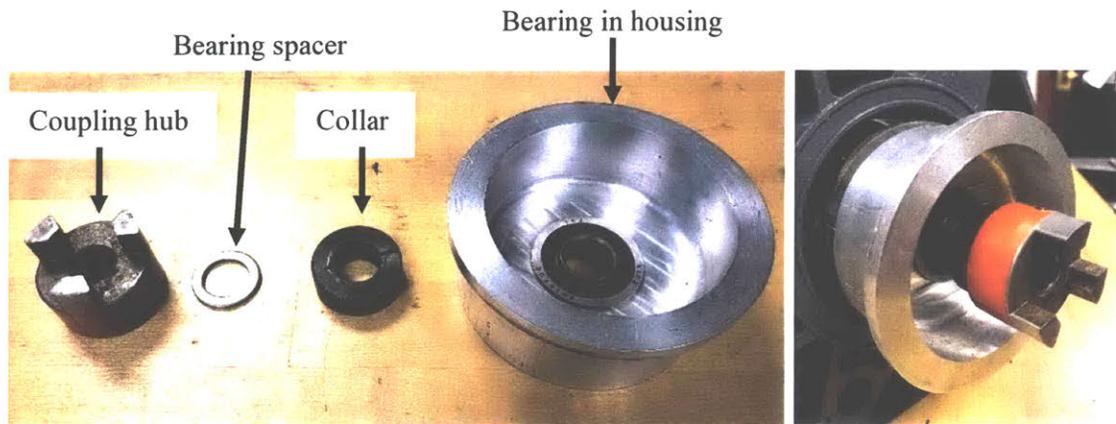
Figure 3-7: Photographs of the bearing module parts (left) and assembly mounted on the shaft end (right). Once this is assembled on the shaft, the collar is tightened, then the shafted is pushed through the pipe until the outer flange on the aluminum bearing housing makes contact with the end of the pipe. The coupling hub on the right mates with an identical coupling on the motor shaft with a hytrel spider as discussed in 3.2 below. When assembled, the bearing spacer is inserted between the collar and bearing to provide a good contact surface to transmit thrust to the bearing.

3.2 Motor and Coupling

The auger is powered by a hydraulic motor mounted at the end of the pipe on the axis of the auger. A hydraulic system was chosen since they are inherently sealed against water and they provide ample power to handle clogs in the pipe. Having no way to accurately predict the torque required to push a clog, the motor was intended to be oversized. A Danfoss OMM 20 motor salvaged from a previous project and was available for use in this project, so to save time and money, this motor was selected. It outputs 300 in-lbs. of torque at 300 RPM with a 1.3 GPM hydraulic flow at 2000 psi. As such, a corresponding SPX model AB-1636 2 HP hydraulic power pack was selected to provide that power. This was expected to be more than enough to tear apart any biomass that may build up in the auger, but hay (which was used to simulate sargassum) proved to be too strong and caused it to stall when it clogged. These results will be further discussed in section 4.2.

30

The motor is mounted to a custom-machined HDPE plate which is bolted to a standard PVC flange which is glued to the end of the pipe past the inlet hole. It may be advantageous to mount the motor off-axis due to geometric constraints in future applications, but that was not necessary for the model that was built for this thesis. This change would require the addition of a gear box or drive chain to transmit torque to the auger.
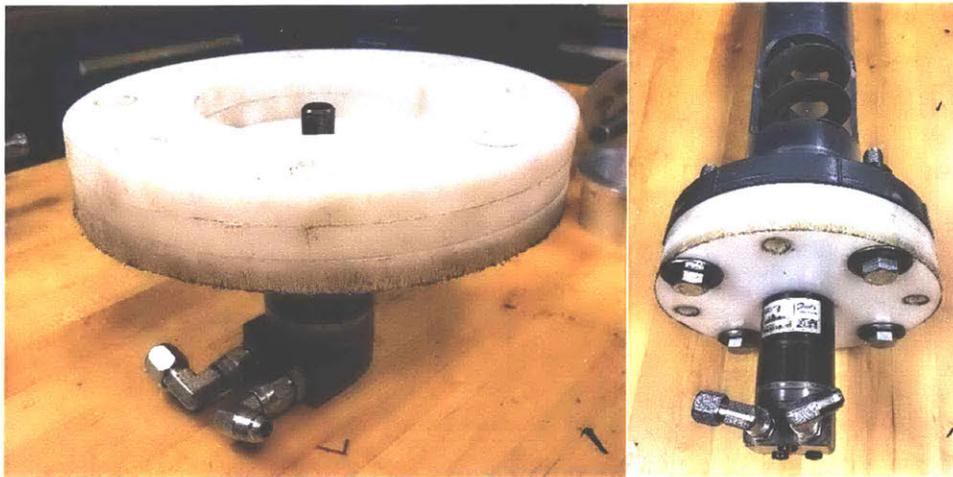
Figure 3-8: Photographs of the motor and mounting plates (left) and this subassembly mounted to the end of the pipe (right). Note that the photograph on the right only shows four bolts holding the plates onto the pipe flange. For testing, all eight bolt holes were used. Also note that the motor's hydraulic ports were pointed out so that the hoses could not obstruct the pipe inlet.

A Lovejoy spider coupling with a hytrel spider was used to couple the motor shaft directly to the 0.75 inch shaft welded to the screw. The flexible hytrel element of the spider coupling accounts for the misalignment that is expected in this assembly. A keyway was cut in the drive shaft so that a key could be used to transmit torque from the coupling to the shaft in the second iteration. Initially, a set screw in the coupling hub was tightened onto a flat surface on the shaft to transmit torque. This was identified as another potential failure point since the set screw is at risk of shearing, so a keyway was added.

3.3 Pipe Selection

For testing this system, it was important to be able to see inside the pipe, to observe how the auger performs and how the sargassum behaves moving through it. The most important objective of the testing stage was to find out if the underlying assumptions for how it would work hold up which requires seeing inside the pipe. For this reason, a clear PVC pipe was used for the length of pipe with the auger in it. PVC provided ample strength and a low enough friction bearing surface. Steel tends to wear down PVC quicker than other plastics, but test runs were not nearly long enough for this to be a concern.
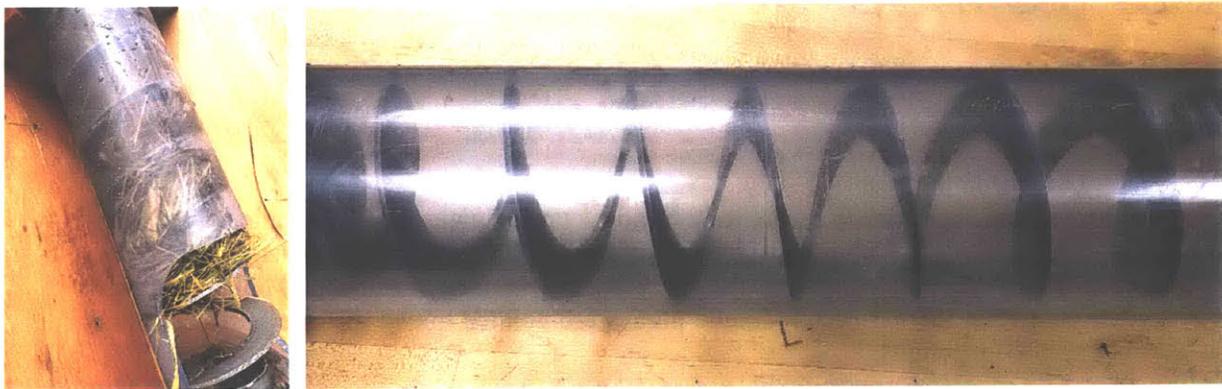
Figure 3-9: Photographs of the clear PVC pipe with hay in it (left) and just the auger (right). Note that the wear from the spinning of the ager started making the inner wall of the pipe less transparent, but that the contents of the pipe are still plainly visible.

Instead of a hanger bearing to support the free end, shaftless augers rely on a plastic liner around the inside of the pipe to act as a bearing surface for the unsupported end of the auger. To provide proper bearing support, the length of contact between the auger and liner must be at least 2 pipe diameters.

For ocean applications, polyethylene would likely be used as a bearing surface due to its low friction and its resistance to wear, corrosion, and water absorption. Ideally, this would be ultra-high molecular weight polyethylene (UHMWPE) if available, but if not, high density polyethylene (HDPE) will be used as a substitute. This pipe can be made either by adding a polyethylene liner to a steel pipe or by using an entirely polyethylene pipe. The full polyethylene pipe is advantageous due to its simplicity, but there may be issues if this pipe cannot be sourced with an inner diameter that fits close around the auger.

For the sake of this test, the inlet was cut out of the side of the pipe near the base of the screw. Augers work best when fed from the side, but this may not be an option in certain inlet devices, so future work may look into different inlet geometries. For instance, there may be a way to feed straight through the end of the tube as long as you can fit a properly supported bearing and a drive mechanism in the center of the pipe without obstructing flow too much.
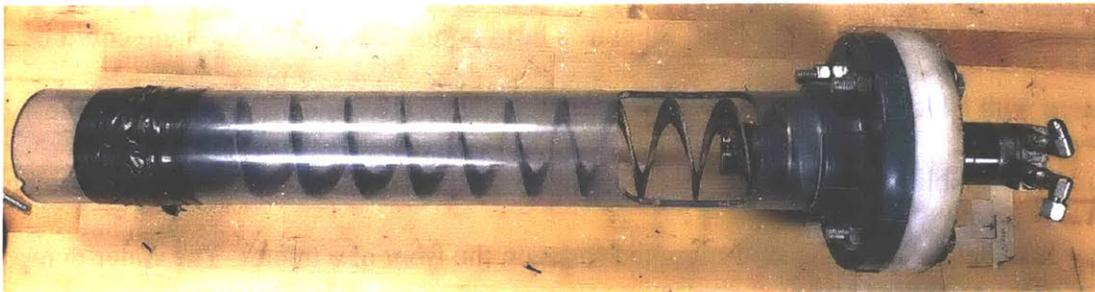
Figure 3-10: Photograph of the full shaftless auger module mounted in the pipe.

3.4 Bill of Materials

Table 3-1 shows a Bill of Materials for the 4" auger module used in the experiment explained below. The total cost of the system was $1259.86. Refer to the part numbers to find the specs of all parts used.

Description	Price ($)	Supplier	Part Number
Auger flighting with 4" OD and 2" ID	199.00	Express Flighting	Made to order
PVC Pipe	115.39	McMaster-Carr	49035K33
PVC Flange	20.67	McMaster-Carr	4881K219
Hydraulic Motor	175.00	Danfoss	OMM 20
Hydraulic Pump	529.25	Surplus Center	SPX AB-1636
Shaft Bearing	16.59	McMaster-Carr	6384K367
Coupling Hubs	22.02	McMaster-Carr	6408K14
Coupling Spider	24.78	McMaster-Carr	6408K95
0.75" OD Drive shaft	17.85	McMaster-Carr	89955K899
2" OD auger shaft	12.91	McMaster-Carr	7767T291
Shaft Collar	2.89	McMaster-Carr	6435K16
HDPE sheet for endplate	48.36	McMaster-Carr	8619K472
Al for bearing housing	33.61	McMaster-Carr	1610T39
Steel Sheet for shaft flange	21.79	McMaster-Carr	8983K128
Fasteners for flange	19.75	Pill Hardware	N/A
Total	**1259.86**		

Table 3-1: Bill of Materials for the 4 inch scale design.

4. Experiment

4.1 Test Setup

This model was tested in Prof. Slocum's farm pond where the full system could be simulated with a large body of water and model vegetation (hay and sargassum from the Dominican Republic that had been dried 7 months). A simple welded steel structure was built to outrigger the device from the skid-mounted forks on the front of a tractor. The water pump, power pack, and hydraulic power unit (for the hydraulic motor) were mounted on the same rig. This structure was lifted and moved about using a John Deer farm tractor with forks mounted instead of the bucket on the front end loader such that the device could be assembled on land, then move it over the pond and lower it into the water at the desired location and depth. A DuroMax XP904WP 9-Hp water pump with a 4 inch inlet was used to pump water up through the suction hose spanning the length of the outrigged arms. The outlet of this pump was pointed

away from the pond such that it was shooting water onto shore to observe the general content of the slurry pumped out of the pond.

The motor used was a Danfoss OMM 20 hydraulic motor powered by an SPX (model AB-1636) 2 HP 1.3 GPM hydraulic power pack with an inline flow adjustment valve. The auger was designed to be removed to get a frame of reference for how it operates with no countermeasures for clogging. To test the auger, the simplest inlet device Gray is investigating was chosen. This device consists of a vee structure with the pipe mounted in the center. This structure is pushed forward through the water to build up a pile of vegetation which is pushed down into the inlet of the pipe by the weight of the pile and the flow of water [1].
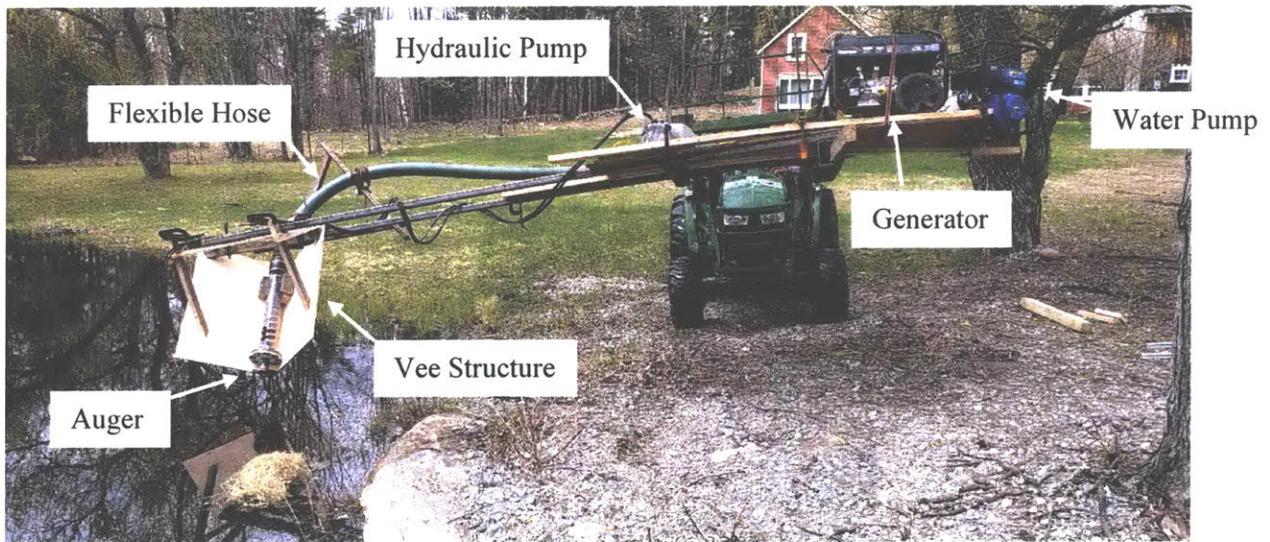
Figure 4-1: The test setup with a vee inlet device mounted to the outrigger held up by a tractor. Note the significant sagging of the outrigger. The weight of the structure to the left caused the beams to bend and the causing that end to dip down toward the water. This did not significantly impact the performance of the system, so it was not fixed in the second iteration.

A limited supply of dried sargassum was available, so straw was used as a substitute to test the basic premise. Straw was tossed into the water in front of the inlet to simulate a high-concentration clump of sargassum. To test the auger in the moving vee inlet, we intended to lay

out a row of floating straw then drive the inlet through it using the tractor, but the error in our test setup made this difficult. It proved quite difficult to keep the depth of the inlet constant while driving the tractor due to the uneven terrain and the flexibility of the support structure. When driving it forward, the elevation of the tractor would change slightly and the cantilevered beam would bounce up and down in response. When this happened, the inlet would come slightly out of the water, letting air in, and the pump would dry run, causing it to quickly shut off. Instead, to simulate a moving inlet, straw was guided toward the inlet using a pitch fork. It was observed that a significant amount of hydraulic fluid floated to the surface of the pond when the motor was lowered into the water (as shown in Figure 4-2). It was not determined whether the motor ports were leaking, or if this was just excess fluid that spilled onto the outside of the motor while it was being installed. Either way, this must be prevented going forward, since this could negatively impact the ecology of the water around it. The hydraulic ports must be sealed tightly and the motor must be cleaned before putting in the water.

Figure 4-2: Photograph of the vee inlet in the water with hay ready to be pushed into it. Note the discoloration of the water in the bottom left corner. This was the hydraulic fluid that got into the pond when the motor was lowered into the water.

4.2 Results and Discussion

When a small concentration of straw was introduced to the flow with the auger, it quickly caught on the flighting, wrapping around it and clinging to the straw around it. As such, the auger worked to slow it down, however it caught too much straw when a larger concentration of straw was introduced. The straw turned out to be too strong and clung too strongly to the straw and walls around it. Some straw pieces caught on the inner edge of the flights, wrapping around them. Some of the straw entering the inlet was caught by the outside edge of the auger, wedging it between the inner wall of the pipe and the auger as it went around. This straw was not able to get past that section of flighting near the inlet. It clung to the straw that was wrapped around the inner edge, forming a clump that the flow could not dislodge. The straw wedged against the wall of the pipe was not cut by the auger as expected, so it jammed, causing the motor to stall. Now there was a dense clog that the auger was not pushing forward, so the pump was not able to pull enough water and came close to running dry.

Figure 4-3: Photographs of the hay clog in the shaftless auger in the pipe (top) and outside of the pipe (bottom).

The straw that was used turned out to be stiffer and stronger than anticipated, causing it to behave quite differently from how sargassum would, as sargassum is not comprised of long strands, but rather more like chopped lettuce. Even without the auger, the straw quickly clogged the water pump itself, so this was not an appropriate test of our system. This told us that it was necessary to use the dried sargassum to get a more accurate idea of how it would behave in the field. The straw tests told us that this system is not suited for stronger, stiffer, stringier species of

vegetation than sargassum. Perhaps it would work if there was less tolerance in the difference between the pipe and auger diameters such that no vegetation could get wedged against the wall, or if the motor was stronger, or if the system was larger relative to the size of the vegetation (as it would be in the full scale design).

When the straw was replaced with the sargassum, it performed much better. The sargassum dried into cohesive mats that stick together much better than live sargassum as shown in Figure 4-4. When it was tossed into the water, much of it just floated at the surface. By pushing it down with a pitch fork, it rehydrated and behaved more like live sargassum, which has weaker buoyancy than straw. In previous tests, Gray determined that rehydrated sargassum has approximately the same viscosity and buoyancy in a fluid as live sargassum, but the dried sargassum was found to be more brittle, with a lower tensile strength. As such, it was less prone to clogs, so further testing with live sargassum is required before the viability of the auger system can be confirmed.

Figure 4-4: Photograph of a mat of dried sargassum before it was wetted. Note that the dry sargassum is cohesive enough to be held up by the sides. They stuck together quite well,

39

but the strands themselves were found to be relatively brittle. Live sargassum does not exhibit this behavior, so further testing must be conducted on live sargassum in the ocean.

When a clump of sargassum got close to the inlet, (often after being pushed down with the pitch fork) it would quickly enter the pipe as a clump and instantly break apart in the auger and flow quickly through the pipe. Only a small amount of sargassum was momentarily caught on the flighting and it was quickly pulled back into the flow. This shows that the flighting has a lower impact on the solids concentration than the model predicted, but that it was quite effective at breaking up this more brittle sargassum. Since the sargassum broke apart so quickly, a clump large enough to induce clogging never formed.

The shafted auger behaved similarly to the shaftless auger, but it experienced much greater suction loss. The flow leaving the pump was much weaker with the shafted auger even before any solids were introduced. When a small amount of hay was added, it wedged against the pipe wall and jammed similar to the shaftless auger. Shafted augers have not been ruled out yet, though. At full scale, with a more optimized geometry, there is no way of knowing if the risk of clogging or cavitation is greater in this system. Since its behavior cannot be predicted, and the two designs are easily interchanged, both designs should be pursued going forward such that one can easily be swapped out for the other.

These tests taught us a lot about how the auger behaves in suction piping and exposed many of the challenges that will be faced going forward in improving the design. Another round of testing with live sargassum will be conducted followed by a full scale extended experiment in the Caribbean.

5. Scaled Design for Extended Experiment

This summer, Gray is setting up a larger-scale extended experiment in the Caribbean in which he will rent a small ship and crew for 20 days to run rigorous high-cycle testing of the full system. An auger module will be designed to be installed in this system in case clogging interrupts these experiments. The minute details of this design are not complete yet, but parts were sized and selected such that a bill of materials including the most critical modules could be developed. This trial is designed around a 5000 GPM pump with a 12 inch diameter inlet. For 20 days, the system will be subjected to approximately 50% utilization, so all parts need to be rated for at least 14400 minutes of service.

In order to greatly extend the lifetime of the pipe, the clear PVC pipe will be replaced with a 12 inch HDPE pipe, or UHMWPE if available. As of yet, a supplier has not been found for a UHMWPE pipe. This will have much greater wear resistance, but it still needs to be monitored for wearing of the bearing surface and a replacement pipe should be prepared before testing in case the wear on the pipe starts to impact performance.

Most of the shaftless auger geometry scales simply from the model previously discussed. The pitch scales directly with the outer diameter. It is standard for the pitch to be available in half of the diameter, so for this system, the pitch will be 6 inches. In initial tests, the inner edge did not catch vegetation as intended and only caused straw to wrap around it, creating clogs in the center. To reduce suction loss and the risk of clogging the center, the inner diameter needs to be scaled up. To make sure the bulk of the flow moves through the center, the area of the center needs to be larger than the area of an auger flight. This requirement leads to the inequality expressed in Equation 5-1, which suggests that the inner diameter needs to be at least 8.5 inches.

$$D_i > \frac{\sqrt{2}}{2} D_o = 0.7 D_o \qquad\qquad 5\text{-}1$$

On the other hand, it is advantageous to decrease the inner diameter of the shafted auger to increase the area that water can flow through around the auger. This will decrease the suction loss in the system. This dimension should be as small as is possible, so the smallest inner diameter available (2.375 inch) was selected. Similarly, a longer pitch, equal to the diameter of the pipe was selected because it opens up the space between the flights, decreasing the minor losses in the auger.

The optimal motor speed was determined using Equation 2-17. For an auger with a 6 inch pitch in a 12 inch pipe, this suggests that the motor should turn at approximately 510 RPM. Ideally, the torque requirement for the motor would be determined based on the load required to push through the sort of clog that caused the 4 inch model to jam and stall. There is no way to predict exactly what will cause clogging at this scale, so it was assumed that it would clog similar to the 4 inch model in which hay wedged against the wall. In order to break through such a clog, the motor must be able to tear a small layer of vegetation in tension, which was conservatively assumed to have the tensile strength of hay (1052 psi [9]). This layer was assumed to be 0.1 inches thick and spans 1 inch of the circumference. In order to overcome the tensile strength of this layer at the pipe wall (radius of 6 inches), the motor must output at least 633 inch-pounds at 510 RPM. This was calculated using Equation 5-2 in which τ refers to the motor torque, σ refers to the tensile strength, A refers to the total area of the layer, and R refers to the radius of the pipe.

$$\tau = \sigma A R \qquad\qquad 5\text{-}2$$

Table 5-1 shows a list of formulas that can be used to select a motor and characterize its performance. In order to meet the load requirements, a 3.6 in³/rev White Drive hydraulic motor was selected. This motor operates at a flow rate of 11 GPM at 1750 psi. To meet these requirements, a 5 HP 208-230/460VAC Hydraulic Power Unit was selected to power this motor.

| Variable	Units	Formula	Calculated Value
Torque (τ)	in-lbs.	$\tau = \sigma A R$ (5-2)	633
Speed (ω)	RPM	$\omega = \dfrac{C_v Q_T}{p A_{pipe}}$ (2-17)	510
Hydraulic Flow Rate (Q_{fluid})	GPM	$Q_{fluid} = \omega d$	7.95
Displacement (d)	in³/rev	$d = \dfrac{Q_{fluid}}{\omega}$	3.6
Pressure (P)	lbs/in²	$P = \dfrac{6.28\tau}{d}$	1104
Power (HP)	HP	$HP = \dfrac{\omega\tau}{63025}$	5.1

Table 5-1: Formulas for hydraulic motor selection

At this scale, the axial load on the bearing is estimated to be 1525 lbs., based on the orifice model. This is a particularly conservative model for an auger with a relatively large inner diameter, but the bearing was still selected based on this number with a safety factor of 4. This bearing is the SKF 6210-2Z sealed stainless steel deep groove ball bearing with a load capacity of 6790 lbs. which is rated for marine applications. Over long periods of heavy use, this bearing will eventually lose its lubrication, so the life of these bearings was estimated using Equation 5-3 below, in which L_{10} refers to how many million revolutions 10% of bearings can take before failing, C refers to the load capacity, and F refers to the load it experiences [10]. For this calculation, it was assumed to take exclusively axial loads, since the auger is designed to transmit radial loads to the pipe. The life was estimated to be around 88.3 million revolutions. Operating at 510 RPM for 14400 minutes, it will run for 7.3 million revolutions, which is only 8% of its estimated life. Operating underwater may speed up the loss of lubrication, so this safety

factor may be necessary. One goal of the experiment is to identify and address any issues with the lifespan of the components of the machine.

$$L_{10} = \left(\frac{C}{F}\right)^3 \qquad\qquad 5\text{-}3$$

To simplify the assembly of the system, the bearing will be moved down to the end of pipe as opposed to being inset into the plug, which made the shaft collar hard to reach. Instead, the motor will be mounted to a machined aluminum part that extends off the cap plate bolted to the pipe flange as shown in Figure 4-4.
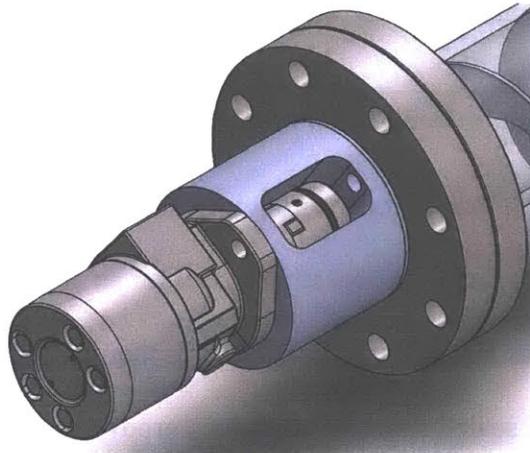
Figure 5-2: CAD model of the new motor mount design. Note the recesses in the sides of the aluminum part which allow access to the bolt holes for mounting it to pipe and the motor.

A bill of materials for this larger-scale version of the design is shown in Table 5-2 below. This shows that the auger module is expected to cost around $4610.37 in total. If this device can effectively eliminate the risk of clogging, then it can save the cost and time of replacing the pump in the case in which it is damaged due to cavitation. The cost of this risk outweighs the cost of the auger, so it makes economic sense to at least prepare this device to be inserted into the system.

Description	Cost per unit ($)	Total Cost of part set ($)	Supplier	Part Number
HDPE Pipe	25 per foot	250	ISCO	N/A
Shaftless Auger with 9" ID and 6" pitch	94 per flight	940	Express Flighting	Made to order
Shafted Auger with a 2.375" ID and 12" pitch	25.86 per foot	129.3	Express Flighting	Made to order
Hydraulic Motor	149.99	149.99	Surplus Center	255060F3169AAAAA
Hydraulic Pump	2,660.49	2,660.49	Grainger	T92C405C93F0-01
Shaft Bearing	74.98	74.98	Motion Industries	SKF 6210-2Z (CN)
Coupling Hub	43.42	130.26	McMaster-Carr	6408K18
Coupling Spider	71.42	71.42	McMaster-Carr	6408K97
Drive shaft	153.75	153.75	McMaster-Carr	7398K25
2.375" OD auger shaft	121.10	121.10	Speedy Metals	N/A
Shaft Collar	29.82	60.64	McMaster-Carr	8386K11
Total		**4610.37**		

Table 5-2: Bill of Materials for the 12 inch design. This was put together to gauge the approximate price of the full system, so it does not include some of the smaller, less expensive parts that will not significantly impact the price of the system

6. Summary and Conclusion

A design was developed for an auger inlet system that reduces the risk of clogging in suction piping for collecting sargassum seaweed from the surface of the ocean. A mathematical model of the system was created, then a small-scale physical model was built to test the assumptions made in the model. These tests exposed flaws in the design, but illustrated the basic viability of the concept, so a full-scale design was concepted to be implemented in an extended field test that will be conducted in the Caribbean this summer. Final design details still need to be completed and onshore testing should be done before deploying to the ocean.

The system did not work when straw, a material significantly stronger than sargassum, was introduced. The straw tangled around the auger in an unexpected way, causing it to clog and stall. When dried sargassum was introduced to the system, it performed much better. With the

limited supply of sargassum available during testing, the pipe did not clog, but the sargassum used was dried, making it brittle even when rehydrated. As such, the system must be tested with live sargassum in the ocean before it can be confirmed that the auger inlet system is the most effective countermeasure to clogging of the suction pipe. Since the solids concentration and pressure losses in the system were not measured during this experiment, it cannot serve as the basis for a completely deterministic, scalable design of the system. Further experiments to measure the quantitative behavior of the system are required in order to create such a deterministic design.

This concept of catching and slowly metering solids that would otherwise cause clogs could be useful for clog prevention in other applications in which a slurry is being pulled through a suction pipe. Augers are simpler and more robust than conveyer belt or chain systems and thus for example, this technology may be necessary for a similar machine that uses suction to pull floating garbage and debris out of the ocean. The system will need more extensive testing at scale before it should be considered for other applications.

7. Bibliography

[1] Gray, L.A., 2019, "Methods for Sequestering Floating Biomass in the Deep Ocean: Sargassum Ocean Sequestration (SOS)," M.S. thesis, Mechanical Engineering, Massachusetts Institute of Technology.

[2] Brackett, R., 2019, "Huge Sargassum Seaweed Blooms Again Threaten Florida, Caribbean and Mexico." from https://weather.com/news/news/2019-01-24-sargassum-blooms-threaten-florida-caribbean-mexico.

[3] Shook, C. A. and Roco, M. C., 1991, *Slurry Flow Principles and Practice*, Butterworth-Heineman, Stoneham, MA.

[4] Bates, L., 1995, *Guide to the Design, Selection, and Application of Screw Feeders*, Professional Engineering Publishing Limited, Suffolk, UK.

[5] 2015, "Discharge Coefficient for Nozzles and Orifices." from https://neutrium.net/fluid_flow/discharge-coefficient-for-nozzles-and-orifices/.

[6] 2012, "Pressure Loss From Fittings – Expansion and Reduction in Pipe Size." from neutrium.net/fluid_flow/pressure-loss-from-fittings-expansion-and-reduction-in-pipe-size/.

[7] Sellens, R., 2012, "Losses in Pipes." from https://me.queensu.ca/People/Sellens/LossesinPipes.html.

[8] Hyde, G., 2018, "Shafted Screw Conveyors vs Shaftless Screw Conveyors." from https://www.jmsequipment.com/shafted-screw-conveyors-vs-shaftless-screw-conveyors/.

[9] O'Dogherty, M.J., Huber, J.A., Dyson, J., Marshall, C.J., 1995, "A Study of the Physical and Mechanical Properties of Wheat Straw," Journal of Agricultural Engineering Research, **62** (2), 133-142.

[10] Slocum, A.H., 1992, Precision Machine Design, Prentice Hall, Upper Saddle River, NJ.